George Vanderheyden
President and CEO

750 E. Pratt Street
14th Floor
Baltimore, Maryland 21202-3106

UniStar
NUCLEAR ENERGY

10 CFR 50.4
10 CFR 52.79

July 31, 2008

ATTN: Document Control Desk
U.S. Nuclear Regulatory Commission
Washington, DC 20555-0001

UN#08-027

Subject: UniStar Nuclear Energy, NRC Docket No. 52-016
Submittal of Supplemental Information for the
Calvert Cliffs Nuclear Power Plant, Unit 3
Combined License Application
Updated Information for Ground Motion Response Spectrum

Reference: Letter from John Rycyna (U.S. NRC) to George Vanderheyden (UniStar Nuclear Energy), "Acceptance Review for Combined License Applications for Calvert Cliffs Nuclear Power Plant, Unit 3," dated June 3, 2008.

In a letter dated June 3, 2008, the U.S. Nuclear Regulatory Commission identified several schedule issues associated with the Calvert Cliffs Nuclear Power Plant (CCNPP) Unit 3 Combined Operating License (COL) Application. This list identified that UniStar Nuclear Energy would submit updated information related to the analysis of the ground motion response spectrum, specifically with regard to the consideration of overburden. This information is provided in the enclosure to this letter and will be incorporated into Revision 4 of the CCNPP Unit 3 COL Application.

If there are any questions regarding this transmittal, please contact Mr. John Price at (410) 470-5531.

D079
NRO

I declare under penalty or perjury that the foregoing is true and correct.

Executed on July 31, 2008

George Vanderheyden

Enclosure: COLA Markup Pages

cc: U.S. NRC Region I
U.S. NRC Resident Inspector, Calvert Cliffs Nuclear Power Plant, Units 1 and 2
NRC Environmental Project Manager, U.S. EPR Combined License Application
NRC Project Manager, U.S. EPR Combined License Application
NRC Project Manager, U.S. EPR Design Certification Application (w/o enclosures)

Enclosure

COLA Markup Pages

below the current ground surface at the CCNPP Unit 3 site. The seismic wave transmission effects of this thick soil column on hard rock ground motions are described in this section.

Section 2.5.2.5.1 is added as a supplement to the U.S. EPR FSAR.

2.5.2.5.1 Development of Site Amplification Functions

2.5.2.5.1.1 Methodology

The calculation of site amplification factors is performed in the following 4 steps:

1. Develop a base-case soil and rock column in which mean low-strain shear wave velocities and material damping values, and strain-dependencies of these properties, are estimated for relevant layers from the hard rock horizon to the surface. At the CCNPP Unit 3 site, hard rock (V_S = 9200 ft/sec (~~2804 m~~~2.8 km/sec) is at a depth of approximately 2600 ft (792 m).

2. Develop a probabilistic model that describes the uncertainties in the above properties, locations of layer boundaries, and correlation between these properties ~~velocities in adjacent layers~~, and generate a set of 60 artificial "randomized" profiles.

3. Use the seismic hazard results at 10^{-4}, 10^{-5}, and 10^{-6} annual frequencies of exceedance to generate smooth spectra, representing LF and HF earthquakes at the ~~two~~three annual frequencies, for input into dynamic response analysis.

4. Use an equivalent-linear site-response formulation together with Random Vibration Theory (RVT) to calculate the dynamic response of the site for each of the 60 artificial profiles, and calculate the mean and standard deviation of site response. This step is repeated for each of the ~~four~~six input motions (10^{-4}, ~~and~~ 10^{-5}, and 10^{-6}, annual frequencies, HF and LF smooth spectra).

   RVT methods characterize the input rock motion using ~~a Fourier amplitude~~ its power spectrum and duration instead of using time domain earthquake input motions. This spectrum is propagated through the soil to the surface using frequency domain transfer functions and computing peak ground accelerations, ~~or~~ spectral accelerations, or peak strains using extreme value statistics. The RVT analysis that was conducted accounted for the strain dependent soil properties in the same manner as time-history methods.

These steps are described in the following subsections.

2.5.2.5.1.2 Base Case Soil/Rock CCNPP Unit 3 and Uncertainties

Development of a base case soil/rock column is described in detail in Section 2.5.4. Summaries of the low strain shear wave velocity, material damping, and strain-dependent properties of the base case materials are provided below in this section. These parameters are used in the site response analyses.

The geology at the CCNPP Unit 3 site consists of marine and fluvial deposits overlying bedrock. The upper 400± ft (122 m) of the site soils was investigated and characterized using test borings, cone penetration testing, test pits, ~~and~~ geophysical methods, and RCTS tests. Information on subsurface conditions below this depth was assembled from available geologic information from various resources ~~and will be discussed later in this section~~.

Natural soils~~Soils~~ in the upper 400 ft (122 m) of the site can generally be divided into the following geotechnical strata:

- Stratum I: Terrace Sand~~, loose to dense~~
- Stratum IIa: Chesapeake Clay/Silt~~, firm to hard~~
- Stratum IIb: Chesapeake Cemented Sand~~, with other sand layers, medium to very dense~~
- Stratum IIc: Chesapeake Clay/Silt~~, stiff to hard~~
- ~~Stratum IIIa: Nanjemoy Cemented Clay/Silt, stiff to hard~~
- Stratum III~~b~~: Nanjemoy Sand~~, dense to very dense~~

Two borings, B-301 and B-401 provide the deepest site-specific soils information collected during the geotechnical investigation for the CCNPP Unit 3 site, and they were also used to obtain the deepest suspension P-S velocity logging profile at the site. The P-S measurements provide shear and compressional wave velocities and Poisson's ratios in soils at 1.6 ft (0.5 m) intervals to a depth of about 400 ft (122 m).

Various available geologic records were reviewed and communications were made with staff at the Maryland Geological Survey, the United States Geological Survey, the Triassic-Jurassic Study Group, Lamont-Doherty Earth Observatory, and Columbia University to develop estimates of subsurface soil properties below 400 ft (122 m) depth. Further details, including associated references, are presented in Subsection 2.5.1. Soils below 400 ft (122 m) consist of Coastal Plain sediments of Eocene, Paleocene, and Cretaceous eras, extending to an estimated depth of about 2555 ft (779 ~~k~~m) below the ground surface. These soils contain sequences of sand, silt, and clay. Given their geologic age, they are expected to be competent soils, consolidated to at least the weight of the overlying soils.

Several available geologic records were reviewed to estimate bedrock characteristics below the site. Various bedrock types occur in the CCNPP Unit 3 site region, including Triassic red beds, Jurassic diabase, granite, schist, and gneiss. However, only granitoid rocks (metamorphic gneiss, schist, or igneous granitic rocks) similar to those exposed in the Piedmont, could be discerned as the potential regional rock underlying the CCNPP Unit 3 site. This rock type was assumed as the predominant rock type at the CCNPP Unit 3 site.

Two sonic profiles were found for wells in the area that penetrated the bedrock, one at Chester, Maryland (about 40 mi (64 km) north of the site) and another at Lexington Park, Maryland (about 10 mi (16 km) south of the site). These two profiles were digitized and converted to shear wave velocity, based on a range of assumed Poisson's ratios for soil and rock.

Unit weights for the soils beneath the site are in the range of about 115 to 120 pcf (pounds per cubic foot) (1765 kg/m^3 to 1929 kg/m^3). The bedrock unit weight was assigned a value of 160 pcf (2592 kg/m^3).

Initially, generic~~Generic~~ EPRI curves from EPRI TR-102293 (EPRI, 1993) were adopted to describe the strain dependencies of shear modulus and damping for subsurface soils. The EPRI "sand" curves cover a depth range up to 1,000 ft (305 m). Since soils at the CCNPP Unit 3 site extend beyond 1,000 feet (305 m), similar curves were extrapolated from the EPRI curves, extending beyond the 1000 ft (305 m), to obtain data for deeper soils. EPRI curves for the upper 400 ft

(122 m) of the site soils were based on available results from the site investigation. Below 400 ft (122 m), a site-specific geologic profile was used as a basis for the soil profiles, including engineering judgment to arrive at the selected EPRI curves. The damping curves for soils were truncated at 15 percent for the initial site response analysis.

Bedrock was assumed to behave elastically with a damping ratio of 1 percent.

Subsequent dynamic laboratory RCTS test results were used to obtain site-specific data on shear modulus and damping characteristics of in situ soils in the upper 400 feet as detailed in Section 2.5.4. A total of 13 undisturbed soil samples, from depths of about 15 ft to about 400 ft below the existing ground surface, were assigned for RCTS testing. The site-specific RCTS-based shear modulus degradation and damping ratio curves were used for the final site amplification factor analysis. Two profiles were evaluated: 1) the entire soil column, including 41 ft of fill above the foundation of the nuclear island and 2) a soil column that did not contain any soil above the base of the nuclear island foundation for the calculation of the GMRS. For the profile including fill, the shear wave for the fill material was assumed to be those of the subsurface strata I and IIa and the shear modulus degradation and damping curves were assumed to be those of subsurface strata I material.

2.5.2.5.1.3 Site Properties Representing Uncertainties and Correlations

To account for variations in shear-wave velocity across the site, 60 artificial profiles were generated using the stochastic model developed by Toro (Toro, 1996), with some modifications to account for conditions at the CCNPP Unit 3 site. These artificial profiles represent the soil column from the top of bedrock (with a bedrock shear-wave velocity of 9,200 ft/s (2804 m/sec) to the ground surface (or to the base of the nuclear island, for the soil column used in the calculation of the GMRS). This model uses as inputs the following quantities:

- The median shear-wave velocity profile, which is equal to the base-case soil and rock profiles described above
- The standard deviation of ln(Vs) (the natural logarithm of the shear-wave velocity) as a function of depth, which is developed using available site and regional data (refer to Section 2.5.4)
- The correlation coefficient between ln(Vs) in adjacent layers, which is taken from generic studies
- The probabilistic characterization of layer thickness as a function of depth, which is also taken from generic studies, and then modified to allow for sharp changes in the base-case velocity profile
- The depth to bedrock, which is randomized to account for epistemic uncertainty in the bedrock-depth data described in Section 2.5.4.
- The median or best-estimate shear stiffness (G/G_{MAX}) and damping curves, which are based on site-specific RCTS tests in the upper 400 feet of the profile (refer to Section 2.5.4).
- The uncertainty in the shear stiffness (G/G_{MAX}) and damping curves.

Figure Figure 2.5-72 shows the median V_S value as a function of depth, and it also shows actual values obtained from boreholes B-301 and B-401 from the P-S velocity logging measurement,

both as recorded and smoothed over a window of 9.8 ft (3 m). The bottom figure in Figure 2.5-72 shows the logarithmic standard deviations calculated from the smoothed data, which were used to generate multiple profiles. Below 400 ft (122 m), data are available from two profiles from Chester and Lexington Park. The shear-wave velocities from these two profiles, and the logarithmic standard deviation computed from them, are shown in Figure 2.5-73.

Values for the standard deviation of ln(Vs) as a function of depth were developed using Vs data from site boreholes B-301 and B-401 (for the top 400 ft of the profile), and from boreholes at Chester and Lexington Park (for greater depths). Refer to Section 2.5.4 for more details on these data.

This study uses the inter-layer correlation model from Toro for ~~category~~ U.S. Geological Survey-category "C" as ~~delineated~~documented in Toro. (Toro, 1996)

The probabilistic characterization of layer thickness consists of a function that describes the rate of layer boundaries as a function of depth. This study utilized a generic form of this function, taken from Toro (Toro, 1996), and then modified to allow for sharp changes in the adopted base-case velocity profile.

Section 2.5.4.7.2.2 indicates that the shear-wave velocity of 9,200 ft/s (2804 m/sec) (for bedrock) is estimated at a depth of approximately 2531 ft (771 m). This value is taken as the base case or median depth. This information on bedrock depth is based on boreholes located tens of miles away from the site where are discussed in Section 2.5.4.7.2.2. The uncertainty associated with depth to bedrock is characterized by a uniform distribution over the interval of 2531 ft(771 m), plus or minus 50 ft (15 m) (the latter number is one half the contouring interval used to estimate the depth to bedrock). Because bedrock occurs at a large depth, the specific details of modeling uncertainty in this depth are not critical to the calculation of site response.

Figure 2.5-74 illustrates the V_S profiles generated for profiles 1 through 10, using the median, logarithmic standard deviation, and correlation model described. These profiles include uncertainty in depth to bedrock. In total, 60 profiles were generated. Figure 2.5-75 compares the median of these 60 V_S profiles to the median V_S profile described in the previous section, indicating excellent agreement. This figure also shows the ±1 standard deviation values of the 60 profiles, reflecting the standard deviations indicated in Figure 2.5-72 and Figure 2.5-73.

Median values of shear stiffness (G/G_{MAX}) and damping for each geologic unit are described in Section 2.5.4. Uncertainties in the properties for each ~~soil unit~~curve-type are characterized using the values obtained by Costantino (Co~~n~~stantino, 1996). In addition, the correlation coefficient between the ln((G/G_{MAX}) and ln(damping) residuals is given a value of 0.75. Figure 2.5-76 and Figure 2.5-77 illustrate the shear stiffness and damping curves generated for one of the geologic units, the Chesapeake silt/clay that is present at the depth range from approximately 100 ft (30 m) to 280 ft (85 m).

This set of 60 profiles, consisting of V_S versus depth, depth to bedrock, stiffness, and damping, are used to calculate and quantify site response and its uncertainty, as described in the following sections.

2.5.2.5.1.4 Development of Low-Frequency and High-Frequency Smooth Spectra

In order to derive smooth spectra corresponding to the 10^{-4} and 10^{-5} amplitudes, the mean magnitudes and distances summarized in Table 2.5-21 were used in the following way. The magnitudes and distances were applied to spectral shape equations from NUREG/CR-6728

(NRC, 2001) to determine realistic spectral shapes for the four representative earthquakes (10^{-4} and 10^{-5}, HF and LF events) – see Figure 2.5-70 and Figure 2.5-71. The HF shapes were scaled to the Uniform Hazard Spectra mean values for 10^{-4} or 10^{-5}, as appropriate, from Table 2.5-24 for 5 Hz, 10 Hz, 25 Hz, and 100 Hz. The shapes were used to interpolate between these 4 structural frequencies. Below 5 Hz, the HF spectral shape was extrapolated from 5 Hz, without regard to Uniform Hazard Spectra amplitudes at lower frequencies. The LF shapes were scaled to the Uniform Hazard Spectra values for 10^{-4} or 10^{-5}, as appropriate, from Table 2.5-24 for 0.5 Hz, 1 Hz, and 2.5 Hz. Below 0.5 Hz the spectral shape was extrapolated from 0.5 Hz. Above 2.5 Hz the spectral shape was extrapolated from 2.5 Hz, without regard to Uniform Hazard Spectra amplitudes at higher frequencies.

Creation of smoothed 10^{-4} and 10^{-5} spectra in this way ensures that the HF spectra match the 10^{-4} and 10^{-5} Uniform Hazard Spectra values at high frequencies (5 Hz and above), and ensures that the LF spectra match the 10^{-4} and 10^{-5} Uniform Hazard Spectra values at low frequencies (2.5 Hz and below). In between calculated values, the spectra have smooth and realistic shapes that reflect the magnitudes and distances dominating the seismic hazard, as reflected in Table 2.5-21.

2.5.2.5.1.5 Site Response Analysis

The site response analysis performed for the CCNPP Unit 3 site used Random Vibration Theory (RVT). The application of RVT to site response has been described by Schneider (Schneider, 1991), Stepp (Stepp, 1991), Silva (Silva, 1997), and Rathje (Rathje, 2006), and a theoretical description of the method will not be presented here. Given a site-specific soil column and the above studies, the fundamental assumptions are as follows:

- The site response can be modeled using horizontal soil layers and a one-dimensional analysis.
- Vertically-propagating shear waves are the dominant contributor to site response.
- An equivalent-linear formulation of soil nonlinearity is appropriate for the characterization of site response.

These are the same assumptions that are implemented in the SHAKE program (Idriss, 1992) and that constitute standard practice for site-response calculations. In this respect, RVT and SHAKE are similar. Both use an iterative, frequency-domain equivalent-linear calculation to determine site response, and the frequency-domain representation of wave propagation in the the layered medium is identical for both approaches. The difference is that RVT works with ground-motion power spectrum (and its relation to the response spectrum and other peak-response quantities), thus representing an ensemble of ground motions, while SHAKE works with individual time histories and their Fourier transforms, thus representing one specific ground motion. Starting from the same inputs (e.g. the site properties described in Section 2.5.2.5.1.3 and the same rock response spectrum), both procedures will lead to similar estimates of site response (see, for example, Rathje (Rathje, 2006)).

The RVT site-response analysis requires the estimation of an additional parameter, strong motion duration, which does not have a strong influence on the calculated site response. Strong motion durations of the rock motions are calculated from the mean magnitudes and distances of the controlling earthquakes as taken from the deaggregation results (see Table 2.5-21). Estimates of strong motion duration depend on crustal shear-wave velocity, , and seismic stress drop, $\Delta\sigma$, as follows:

$$T = \frac{1}{f_c} + 0.05R \qquad \text{Eq. 2.5.2-1}$$

where R is the distance of controlling earthquake and earthquake corner frequency f_c is defined as:

$$fc = 4.9 \times 10^6 \beta \left(\frac{\Delta\sigma}{M_0}\right)^{1/3}$$

~~and~~

$$M_0 = 10^{(1.5\mathbf{M} + 16.05)}$$

where M_0 is the seismic moment and **M** is the moment magnitude of the controlling earthquake (Rathje, 2006). A value of 3.5 km/s was used for β and 120 bars for $\Delta\sigma$, reflecting eastern US conditions.

One parameter that is used by both the RVT method and SHAKE is the effective strain ratio. This parameter is estimated using the expression (**M**-1)/10 (Idriss, 1992), where **M** is the magnitude of the controlling earthquake taken from the deaggregation analysis. A value of 0.5, rather than 0.45, was used for the 10^{-4}, 10^{-5}, and 10^{-6} HF runs to remain within the 0.5 - 0.7 range found empirically by Kramer (Kramer, 1996). Values of 0.58, ~~and~~ 0.59, and 0.61, derived from Idriss (Irdriss, 1992) formula, were used for the 10^{-4}, ~~and~~ 10^{-5}, and 10^{-6} LF runs. As is the case for strong motion duration, computed site response is not very sensitive to estimates of effective strain ratio.

The RVT method starts with the response spectrum of rock motion (for example, the 10^{-4} HF spectrum). It then generates a Fourier spectrum corresponding to that input response spectrum, using an estimate of strong motion duration (calculated as described above) as an additional input. This step is denoted as the Inverse RVT (or IRVT) step. An iterative procedure (similar to that in SHAKE) is then applied to calculate peak and effective shear strains in each layer using RVT, update the stiffness and damping in each layer using the calculated effective strains and the G/G_{max} and damping curves for the layer, and repeat the process until it converges. The final (or strain-compatible) stiffness and damping are then used to calculate the strain-compatible site transfer function. This transfer function is then multipled by the Fourier spectrum of the input rock motion to obtain the Fourier spectrum of the motion at the top of ~~soil~~profile ~~or at the desired elevation (in this case at 41 ft depth~~ for either outcrop ~~or~~ in-column conditions), from which ~~the 41 ft depth outcrop~~ response spectra~~spectrum~~ ~~is~~are calculated using RVT.

This process is repeated multiple times, once for each ~~set of simulated~~artificial profile ~~parameters~~. For sixty site profiles, sixty ~~41 ft depth outcrop~~ response spectra are calculated, from which statistics of site response are obtained.

~~As an example, Figure 2.5-78 shows 60 site spectra (41 ft depth outcrop) calculated for the 10^{-4} HF input motion, along with the median spectrum (shown as the red curve). The heavy curve at the bottom shows the calculated logarithmic standard deviation from the 60 response spectra, plotted with values shown on the right axis of the figure. Across all frequencies, logarithmic standard deviations are in the range 0.15 to 0.30.~~

~~In addition, t~~The above calculations are repeated multiple times, once for each input rock spectrum. Thus the site response is calculated separately for the 10^{-4} HF, 10^{-4} LF, 10^{-5} HF, 10^{-5} LF, 10^{-6} HF, and 10^{-6} LF spectra.

In comparison to the SHAKE approach, the RVT approach avoids the requirement of performing spectral matching on the input time histories to match an input rock spectrum, and avoids analyzing each individual time history with a site-response program.

The site amplification factor is defined as the ~~41 ft depth outcrop~~surface response spectral amplitude at each frequency, computed using the set of profiles that do not contain the 41 feet of fill above the nuclear island, divided by the input rock spectral amplitude. Figure 2.5-78 shows the logarithmic mean and standard deviation of site amplification factor ~~at 41 ft depth~~ from the 60 profiles for the 10^{-4} HF input motion. As would be expected by the large depth of sediments at the site, amplifications are largest at low frequencies, and de-amplification occurs at high frequencies because of soil damping. The maximum strains in the soil column are low for this motion, and this is shown in Figure 2.5-79, which plots the maximum strains calculated for the 60 profiles versus depth. Maximum strains are generally less than 0.01 percent, with some profiles having strains in shallow layers up to 0.03 percent.

Figure 2.5-80 and Figure 2.5-81 show similar plots of amplification factors and maximum strains for the 10^{-4} LF motion. The results are similar to those for the HF motion, with the soil column generally exhibiting maximum strains less than 0.01 percent.

Figure 2.5-82 through Figure 2.5-85 show comparable plots of amplification factors and maximum strains for the 10^{-5} input motion, both HF and LF. For this higher motion, larger maximum strains are observed, but they are still generally less than 0.03 percent. A few profiles exhibit maximum strains of about 0.1 percent at shallow depths. These strains are within the range for which the equivalent linear site response formulation has been validated.

Table 2.5-23 documents the mean amplification factors for 10^{-4}, 10^{-5}, and ~~10^{-56}~~ rock input motions, and for HF and LF spectra.~~}~~

2.5.2.6 Ground Motion Response Spectra

The U.S. EPR FSAR includes the following COL Item in Section 2.5.2.6:

> A COL applicant that references the U.S. EPR design certification will verify that the site-specific seismic parameters are enveloped by the CSDRS (anchored at 0.3 g PGA) and the 10 generic soil profiles discussed in Section 2.5.2 and Section 3.7.1 and summarized in Table 3.7.1-6.

This COL Item is addressed as follows:

This section and Section 3.7.1 describes the reconciliation of the site-specific parameters for CCNPP Unit 3 and demonstrates that these parameters are enveloped by the Certified Seismic Design Response Spectra (CSDRS), anchored at 0.3 g PGA, and the 10 generic soil profiles used in the design of the U.S. EPR.

Table 5.0-1 of the U.S. EPR FSAR identifies shear wave velocity as a required parameter to be enveloped, defined as "Minimum shear wave velocity of 1000 feet per second (Low strain best estimate average value at bottom of basemat)."

Table 2.5-21—{Mean Magnitudes and Distances from Deaggregations}

Struct. frequency	Annual Freq. Exceed.	Overall hazard		Hazard from R<100 km		Hazard from R>100 km	
		M	R, km	M	R, km	M	R, km
1 & 2.5 Hz	1E-4	6.3	300	5.6	39	6.8	430
5 & 10 Hz	1E-4	5.5	97	5.5	35	6.2	220
1 & 2.5 Hz	1E-5	6.3	220	5.8	27	6.9	450
5 & 10 Hz	1E-5	~~5.5~~5.4	35	5.5	18	6.5	~~193~~190
1 & 2.5 Hz	1E-6	6.2	120	5.9	18	7.1	460
5 & 10 Hz	1E-6	5.5	17	5.6	11	6.8	160

Table 2.5-22—{Recommended Horizontal and Vertical SSE and OBE Amplitudes and Common V/H Ratios}

Freq	Horizontal SSE (g)	Vertical SSE (g)	Horizontal OBE (g)	Vertical OBE (g)	V/H
0.1	2.672.70E-03	2.002.03E-03	8.919.00E-04	6.686.75E-04	0.75
0.125	4.694.70E-03	3.52E-03	1.561.57E-03	1.17E-03	0.75
0.15	7.847.85E-03	5.885.89E-03	2.612.62E-03	1.96E-03	0.75
0.2	1.792.02E-02	1.341.52E-02	5.976.74E-03	4.485.05E-03	0.75
0.3	2.663.35E-02	1.992.51E-02	8.86E-031.12E-02	6.648.36E-03	0.75
0.4	3.353.57E-02	2.512.68E-02	1.121.19E-02	8.388.93E-03	0.75
0.5	4.494.25E-02	3.373.19E-02	1.501.42E-02	1.121.06E-02	0.75
0.6	6.666.73E-02	5.005.04E-02	2.222.24E-02	1.671.68E-02	0.75
0.7	7.638.19E-02	5.726.14E-02	2.542.73E-02	1.912.05E-02	0.75
0.8	7.929.14E-02	5.946.85E-02	2.643.05E-02	1.982.28E-02	0.75
0.9	8.429.55E-02	6.327.16E-02	2.813.18E-02	2.112.39E-02	0.75
1.	8.79E-021.03E-01	6.597.69E-02	2.933.42E-02	2.202.56E-02	0.75
1.25	9.53E-021.23E-01	7.159.23E-02	3.184.10E-02	2.383.08E-02	0.75
1.5	9.98E-021.28E-01	7.489.64E-02	3.334.28E-02	2.493.21E-02	0.75
2.	1.05E-011.23E-01	7.889.26E-02	3.504.11E-02	2.633.09E-02	0.75
2.5	1.16E-011.29E-01	8.679.70E-02	3.854.31E-02	2.893.23E-02	0.75
3.	1.32E-011.51E-01	9.93E-021.14E-01	4.415.05E-02	3.313.78E-02	0.75
4.	1.44E-011.69E-01	1.081.27E-01	4.795.63E-02	3.594.23E-02	0.75
5.	1.601.72E-01	1.201.29E-01	5.325.75E-02	3.994.31E-02	0.75
6.	1.651.80E-01	1.281.40E-01	5.506.01E-02	4.284.68E-02	0.778
7.	1.651.72E-01	1.331.38E-01	5.515.73E-02	4.424.60E-02	0.802
8.	1.591.64E-01	1.311.35E-01	5.295.46E-02	4.364.49E-02	0.823
9.	1.511.57E-01	1.271.32E-01	5.035.23E-02	4.234.40E-02	0.841
10.	1.451.50E-01	1.241.28E-01	4.824.99E-02	4.134.28E-02	0.858
12.5	1.321.38E-01	1.181.23E-01	4.404.59E-02	3.934.10E-02	0.892
15.	1.191.28E-01	1.101.18E-01	3.984.27E-02	3.673.93E-02	0.921
20.	9.62E-021.09E-01	9.29E-021.05E-01	3.213.62E-02	3.103.50E-02	0.965
25.	8.398.80E-02	8.398.80E-02	2.803.27E-02	2.803.27E-02	1
30.	7.658.77E-02	7.658.77E-02	2.552.92E-02	2.552.92E-02	1
35.	7.268.27E-02	7.26E-028.27E-02	2.422.76E-02	2.42E-022.76E-02	1
40.	7.037.97E-02	7.03E-027.97E-02	2.342.66E-02	2.34E-022.66E-02	1
45.	6.907.81E-02	6.90E-027.81E-02	2.302.60E-02	2.30E-022.60E-02	1
50.	6.837.73E-02	6.83E-027.73E-02	2.282.58E-02	2.28E-022.58E-02	1
60.	6.767.63E-02	6.76E-027.63E-02	2.252.54E-02	2.25E-022.54E-02	1
70.	6.737.59E-02	6.73E-027.59E-02	2.242.53E-02	2.24E-022.53E-02	1
80.	6.717.57E-02	6.71E-027.57E-02	2.242.52E-02	2.24E-022.52E-02	1
90.	6.707.56E-02	6.70E-027.56E-02	2.232.52E-02	2.23E-022.52E-02	1
100.	6.707.55E-02	6.707.55E-02	2.232.52E-02	2.232.52E-02	1

Table 2.5-23—{Calvert Cliffs Site} Amplification Factors for 10^{-4} and 10^{-5} Input Motions and HF and LF Rock Spectra}

Freq. (Hz)	10^{-4} HF	10^{-4} LF	10^{-5} HF	10^{-5} LF
0.1	~~2.09~~2.36	~~1.43~~1.45	~~2.19~~2.52	~~1.44~~1.45
0.125	~~2.01~~2.22	~~1.64~~1.66	~~2.05~~2.31	1.68
0.15	~~2.15~~2.32	~~1.98~~1.99	~~2.17~~2.38	2.05
0.2	~~2.86~~3.25	~~2.88~~3.21	~~2.82~~3.24	~~2.89~~3.27
0.3	~~2.45~~3.06	~~2.42~~3.03	~~2.39~~2.99	~~2.29~~2.89
0.4	~~1.77~~1.94	~~1.71~~1.86	~~1.78~~1.92	~~1.67~~1.78
0.5	~~1.98~~1.92	~~1.89~~1.79	~~2.04~~1.95	~~1.91~~1.81
0.6	~~2.59~~2.65	~~2.51~~2.52	~~2.61~~2.67	~~2.47~~2.49
0.7	~~2.70~~2.94	~~2.64~~2.84	~~2.67~~2.89	~~2.54~~2.73
0.8	~~2.60~~3.01	~~2.56~~2.94	~~2.56~~2.96	~~2.44~~2.82
0.9	~~2.62~~2.99	~~2.56~~2.92	~~2.56~~2.92	~~2.45~~2.77
1	~~2.67~~3.10	~~2.61~~3.03	~~2.55~~3.02	~~2.44~~2.85
1.25	~~2.47~~3.21	~~2.41~~3.16	~~2.29~~3.07	~~2.15~~2.94
1.5	~~2.03~~2.64	~~1.99~~2.61	~~1.88~~2.50	~~1.78~~2.40
2	~~1.63~~1.86	~~1.60~~1.85	~~1.53~~1.76	~~1.45~~1.70
2.5	~~1.62~~1.63	~~1.57~~1.61	~~1.48~~1.53	~~1.38~~1.47
3	~~1.66~~1.71	~~1.59~~1.67	~~1.45~~1.59	~~1.34~~1.51
4	~~1.33~~1.66	~~1.28~~1.61	~~1.14~~1.48	~~1.04~~1.39
5	~~1.24~~1.29	~~1.18~~1.25	~~1.04~~1.13	~~0.93~~1.06
6	~~1.17~~1.21	~~1.09~~1.18	~~0.93~~1.03	~~0.83~~0.97
7	~~1.08~~1.06	~~1.01~~1.03	~~0.84~~0.88	~~0.74~~0.83
8	~~0.98~~0.94	~~0.91~~0.92	~~0.73~~0.77	~~0.65~~0.73
9	~~0.88~~0.85	~~0.82~~0.83	~~0.65~~0.69	~~0.57~~0.66
10	~~0.81~~0.77	~~0.75~~0.77	~~0.58~~0.62	~~0.52~~0.60
12.5	~~0.67~~0.62	~~0.63~~0.64	~~0.45~~0.48	~~0.42~~0.50
15	~~0.56~~0.53	~~0.54~~0.56	~~0.36~~0.40	~~0.37~~0.44
20	~~0.40~~0.40	~~0.42~~0.47	~~0.26~~0.30	~~0.31~~0.37
25	~~0.33~~0.34	~~0.38~~0.42	~~0.21~~0.26	~~0.28~~0.35
30	~~0.29~~0.31	~~0.35~~0.39	~~0.20~~0.23	~~0.27~~0.33
35	~~0.28~~0.29	~~0.34~~0.38	~~0.19~~0.23	~~0.27~~0.33
40	~~0.28~~0.29	~~0.34~~0.38	~~0.20~~0.23	~~0.28~~0.33
45	~~0.29~~0.30	~~0.35~~0.39	~~0.21~~0.24	~~0.28~~0.34
50	~~0.30~~0.32	~~0.36~~0.41	~~0.22~~0.25	~~0.30~~0.36
60	~~0.36~~0.37	~~0.41~~0.46	~~0.26~~0.30	~~0.34~~0.41
70	~~0.44~~0.46	~~0.49~~0.55	~~0.32~~0.36	~~0.41~~0.49
80	~~0.53~~0.56	~~0.58~~0.65	~~0.38~~0.44	~~0.48~~0.58
90	~~0.62~~0.65	~~0.66~~0.74	~~0.45~~0.51	~~0.55~~0.66
100	~~0.69~~0.73	~~0.72~~0.81	~~0.50~~0.57	~~0.60~~0.72

Figure 2.5-72—{Shear Wave Velocity (V_S) and Its Logarithmic Standard Devision for the Top 140 m}

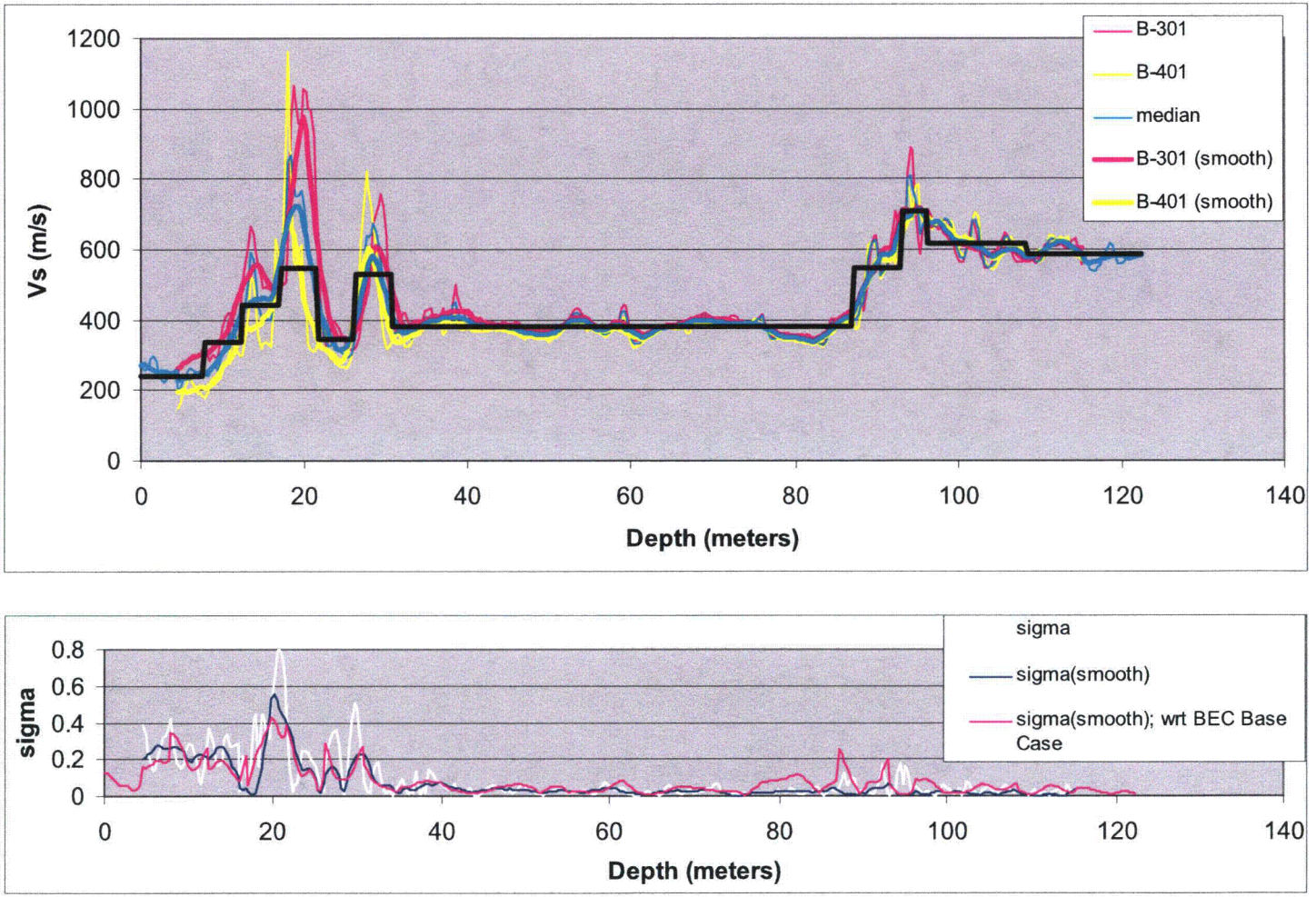

Figure 2.5-74—{Shear-Wave Velocity (Vs) vs Depth or Profiles 1 through 10}

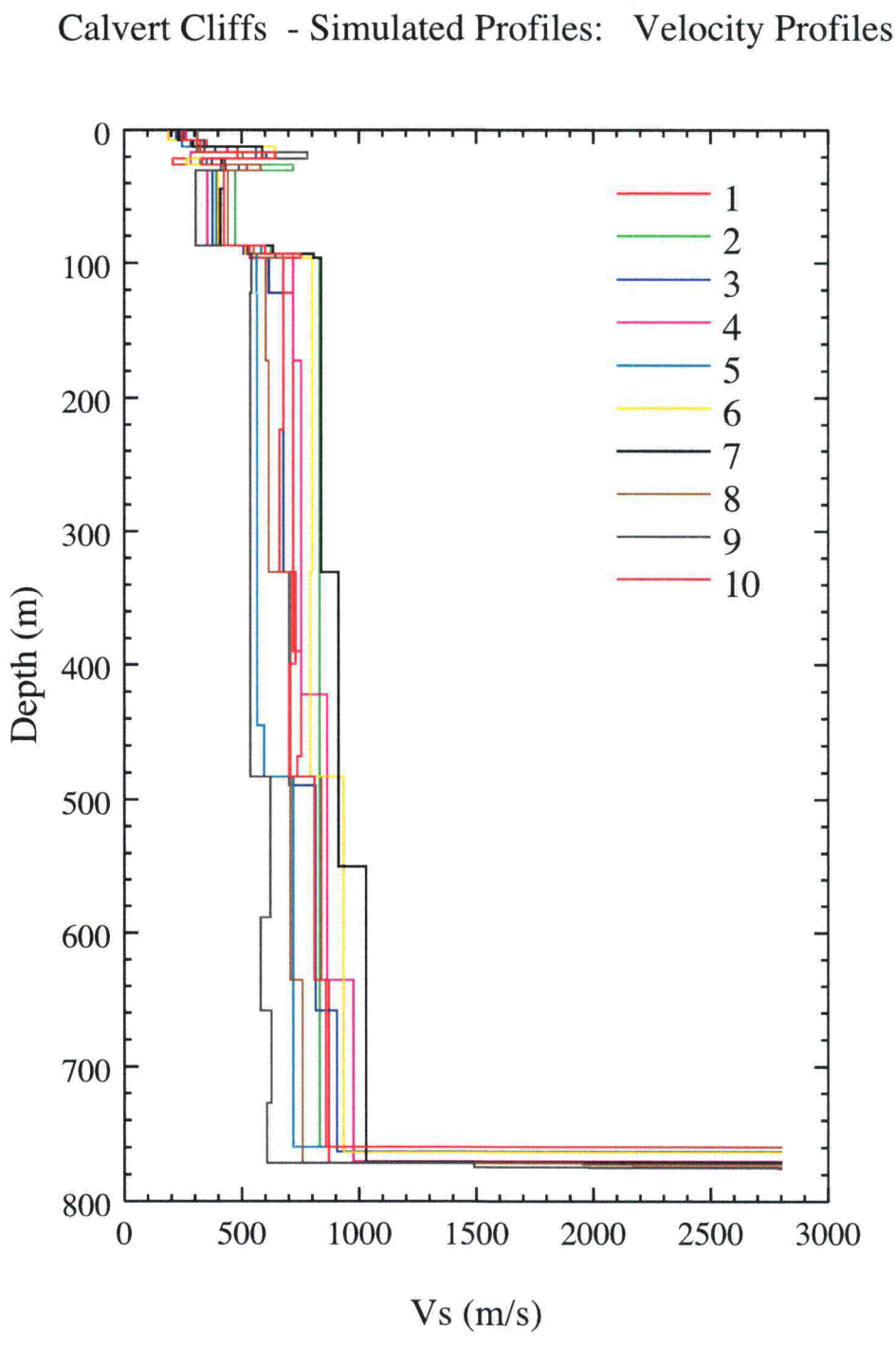

Figure 2.5-75—{Median (Mean of Logarithmic Values) ±Standard Deviation (σ of Log Values) of Shear Wave Velocity (V_S) vs Depth for All 60 Profiles (Thin Solid and Dashed Lines, Compared to Median V_S Profile (red)}

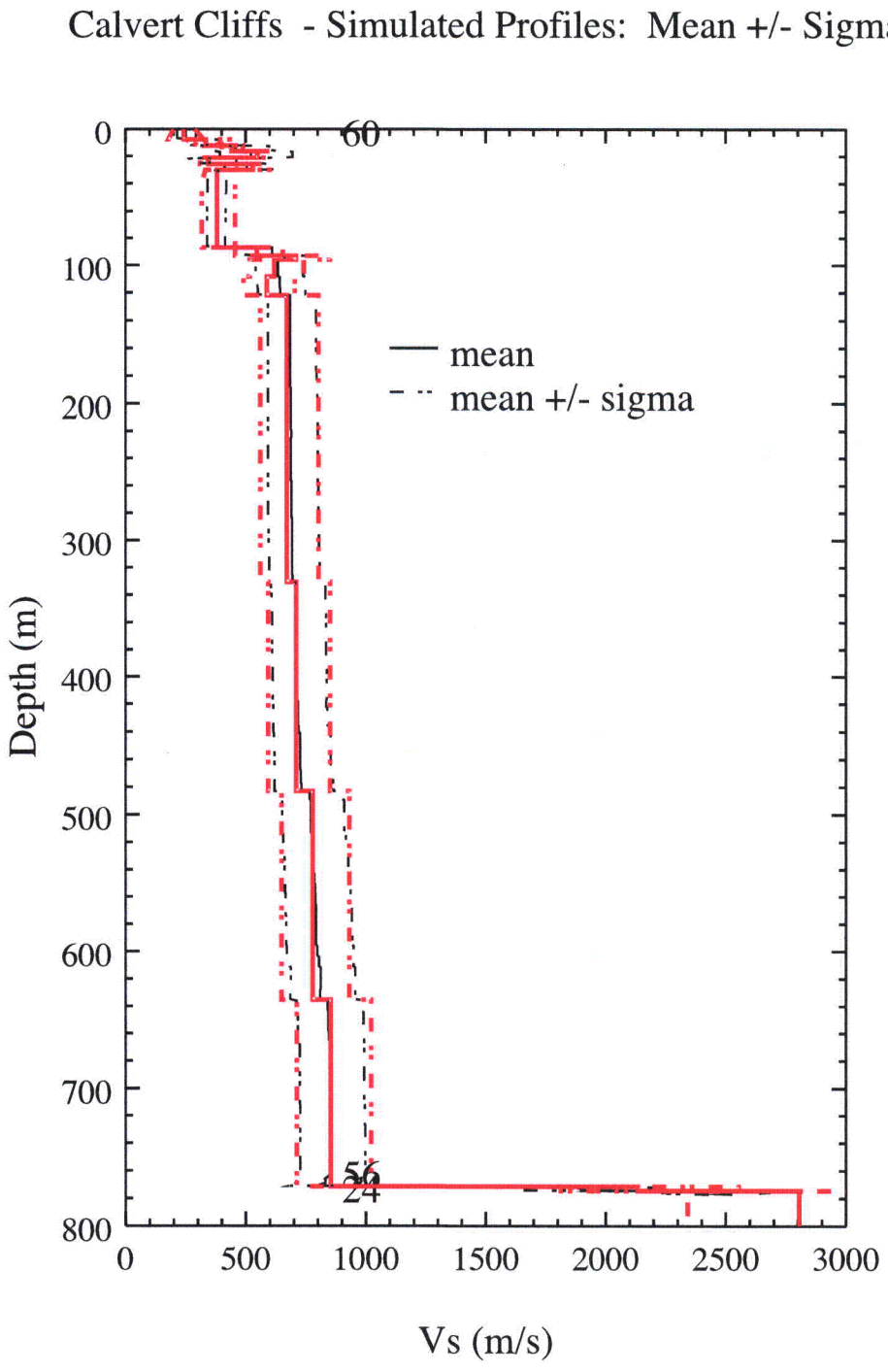

Figure 2.5-76—{G/G_{max} Curves Representing Uncertainty in Shear Stiffness for Soil Type 2 (Chesapeake Clay/Silt)}

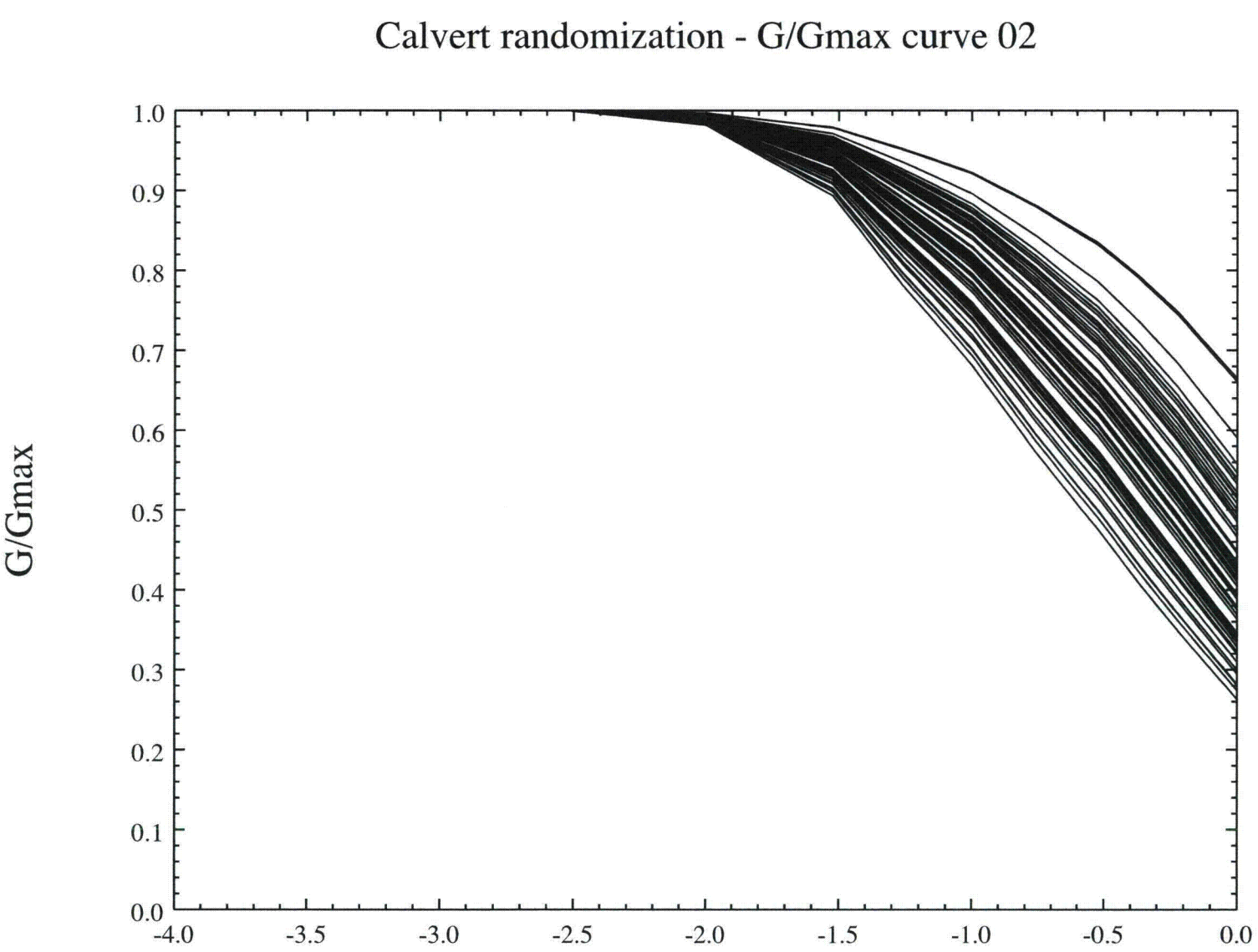

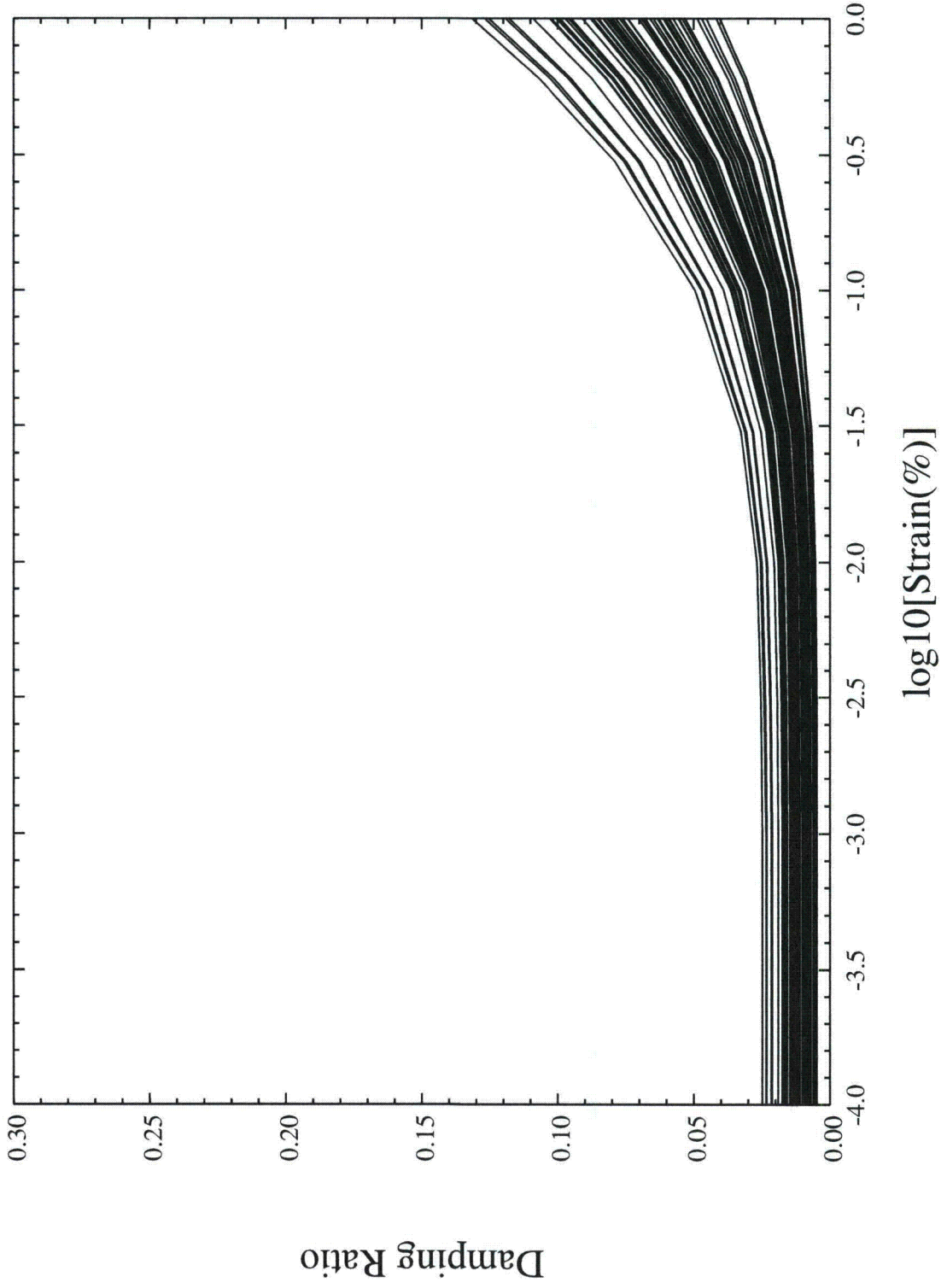

Figure 2.5-77—{Damping Curves Representing Uncertainty in Damping for Soil Type 2 (Chesapeake Clay/Silt)}

Figure 2.5-78—{Logarithmic Mean Site Amplification Factor and Standard Deviation at the Top of a Soil Column with no Backfill for 10^{-4} HF Input Motion}

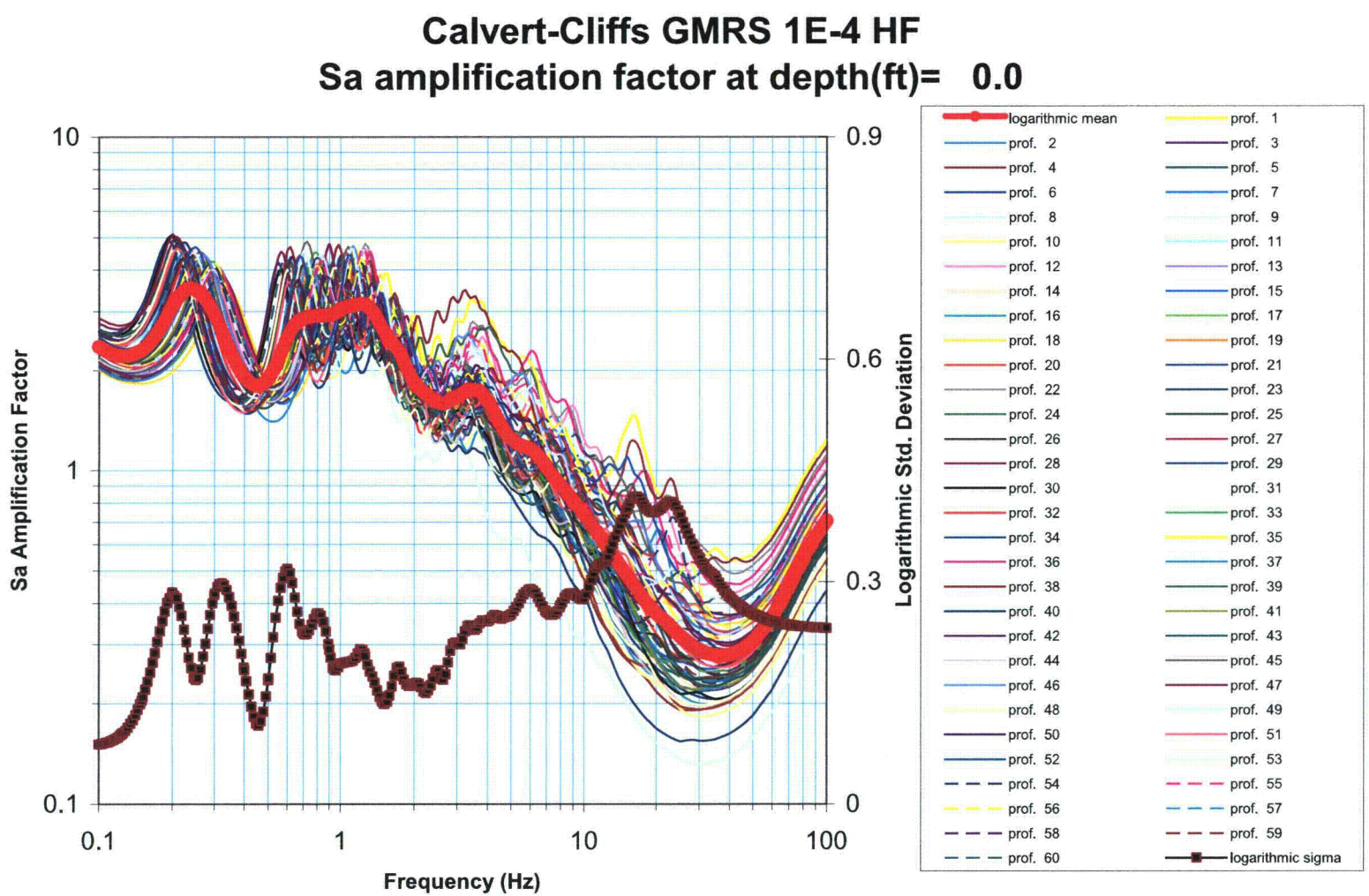

FSAR Section 2.5

Figure 2.5-79—{Maximum Strains vs. Depth for 10^{-4} HF Input Motion}

FSAR Section 2.5

Figure 2.5-80—{Logarithmic Mean Site Amplification Factor and Standard Deviation at the Top of a Soil Column with no Backfill for 10^{-4} LF Input Motion}

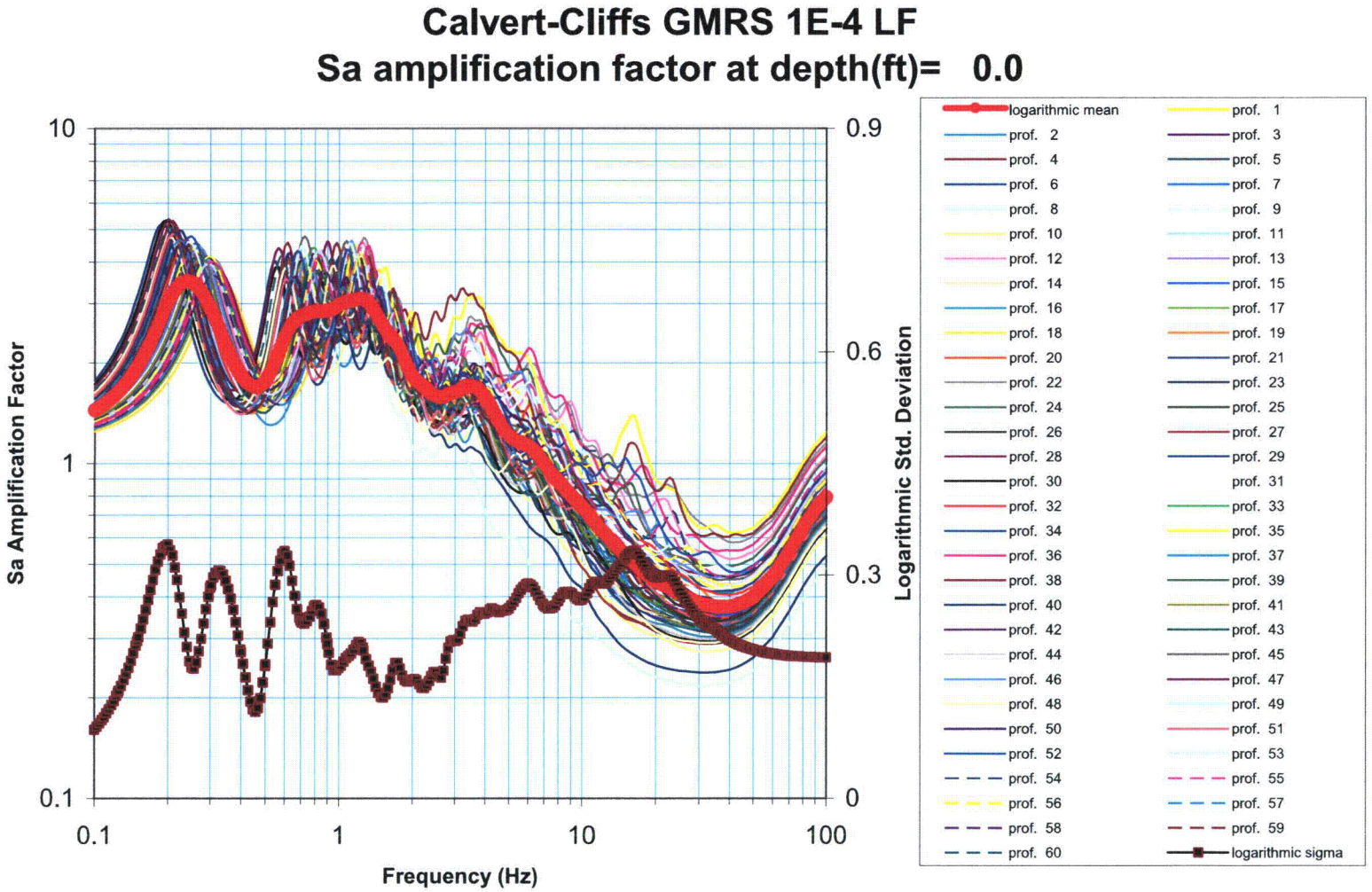

FSAR Section 2.5

Figure 2.5-81—{Maximum Strains vs. Depth for 10^{-4} LF Input Motion}

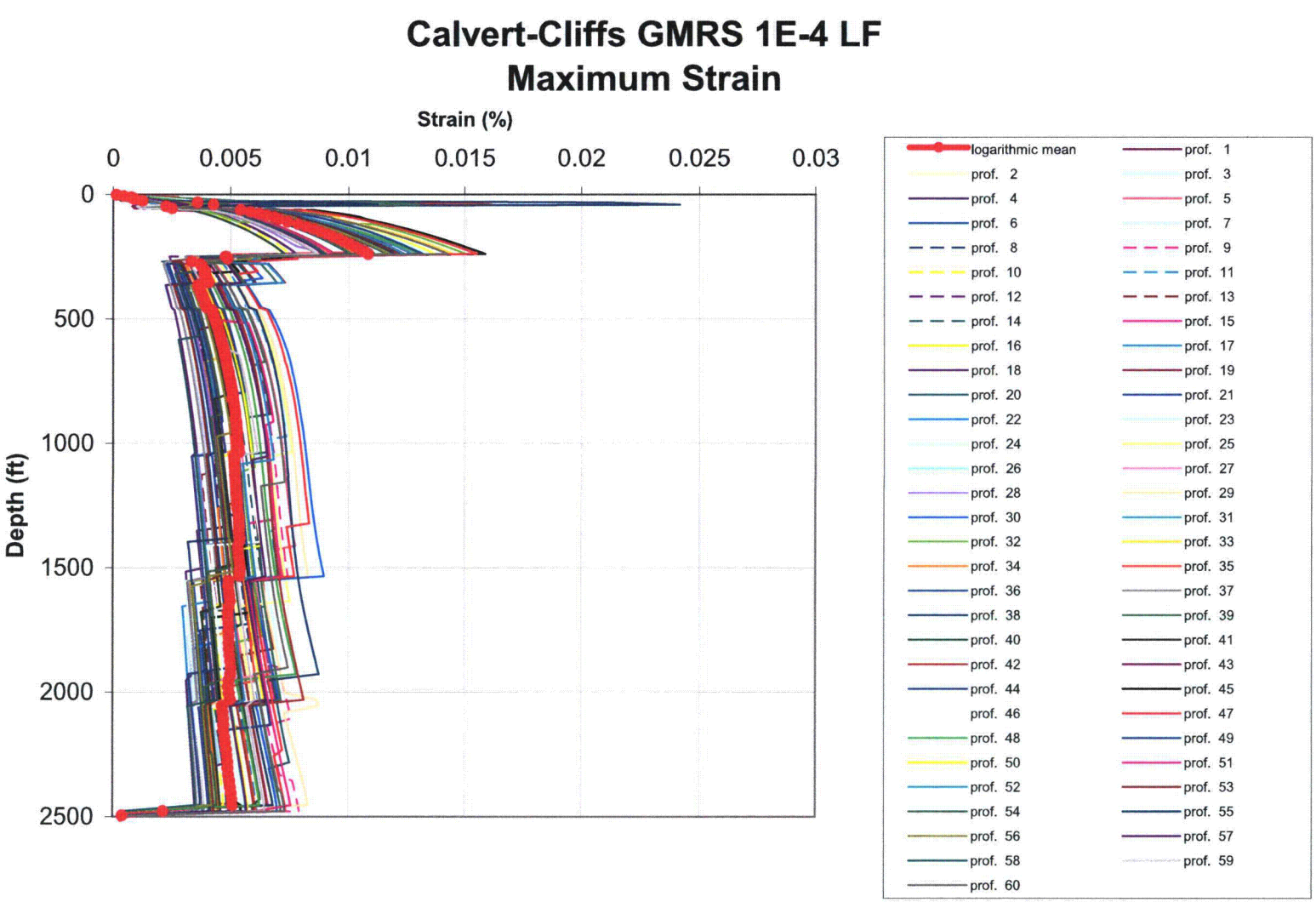

FSAR Section 2.5

Figure 2.5-82—{Logarithmic Mean Site Amplification Factor and Standard Deviation at the Top of a Soil Column with no Backfill for 10^{-5} LF Input Motion}

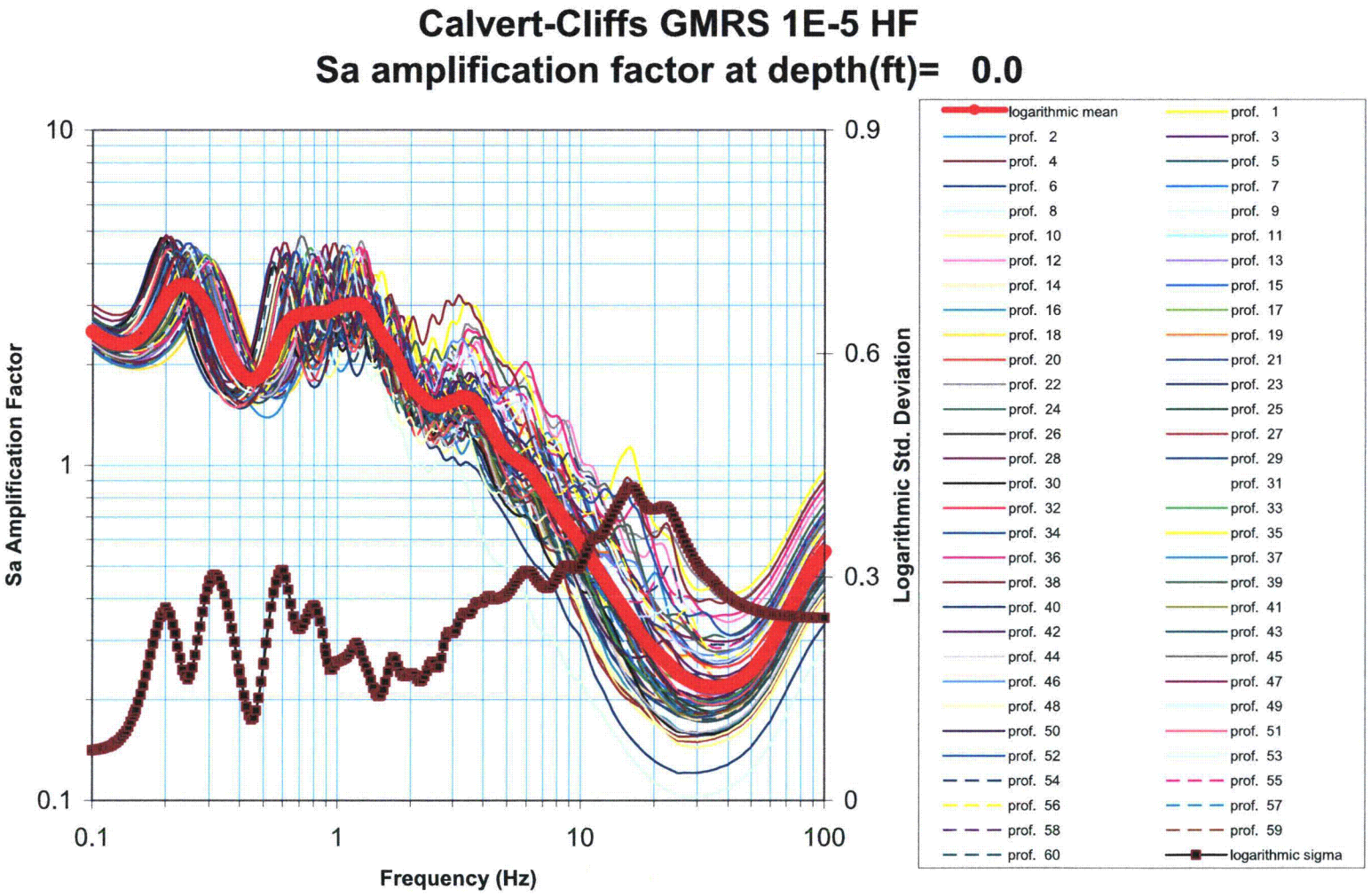

FSAR Section 2.5

Figure 2.5-83—{Maximum Strains vs. Depth for 10^{-5} HF Input Motion}

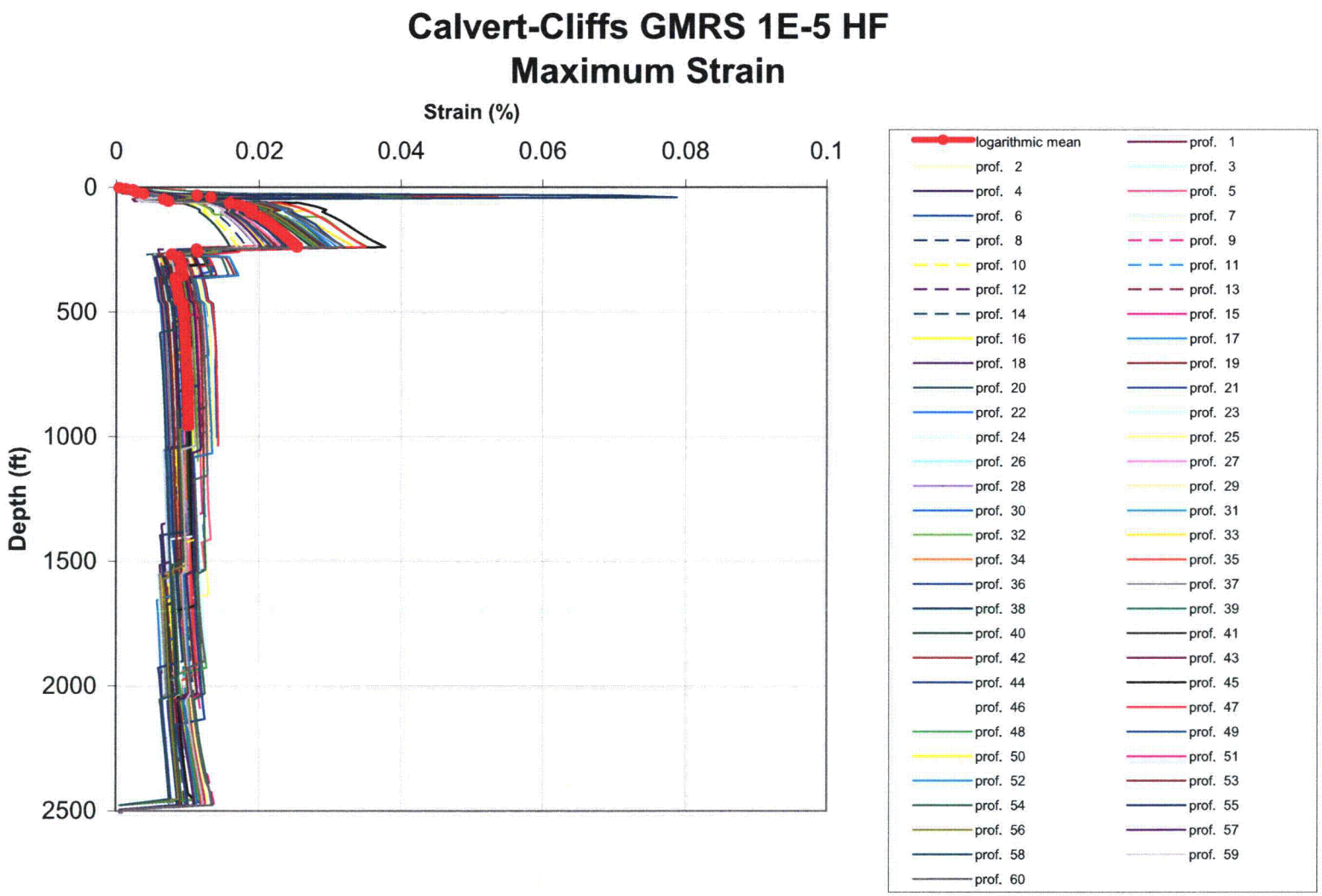

FSAR Section 2.5

Figure 2.5-84—{Logarithmic Mean Site Amplification Factor and Standard Deviation at the Top of a Soil Column with no Backfill for 10^{-5} LF Input Motion}

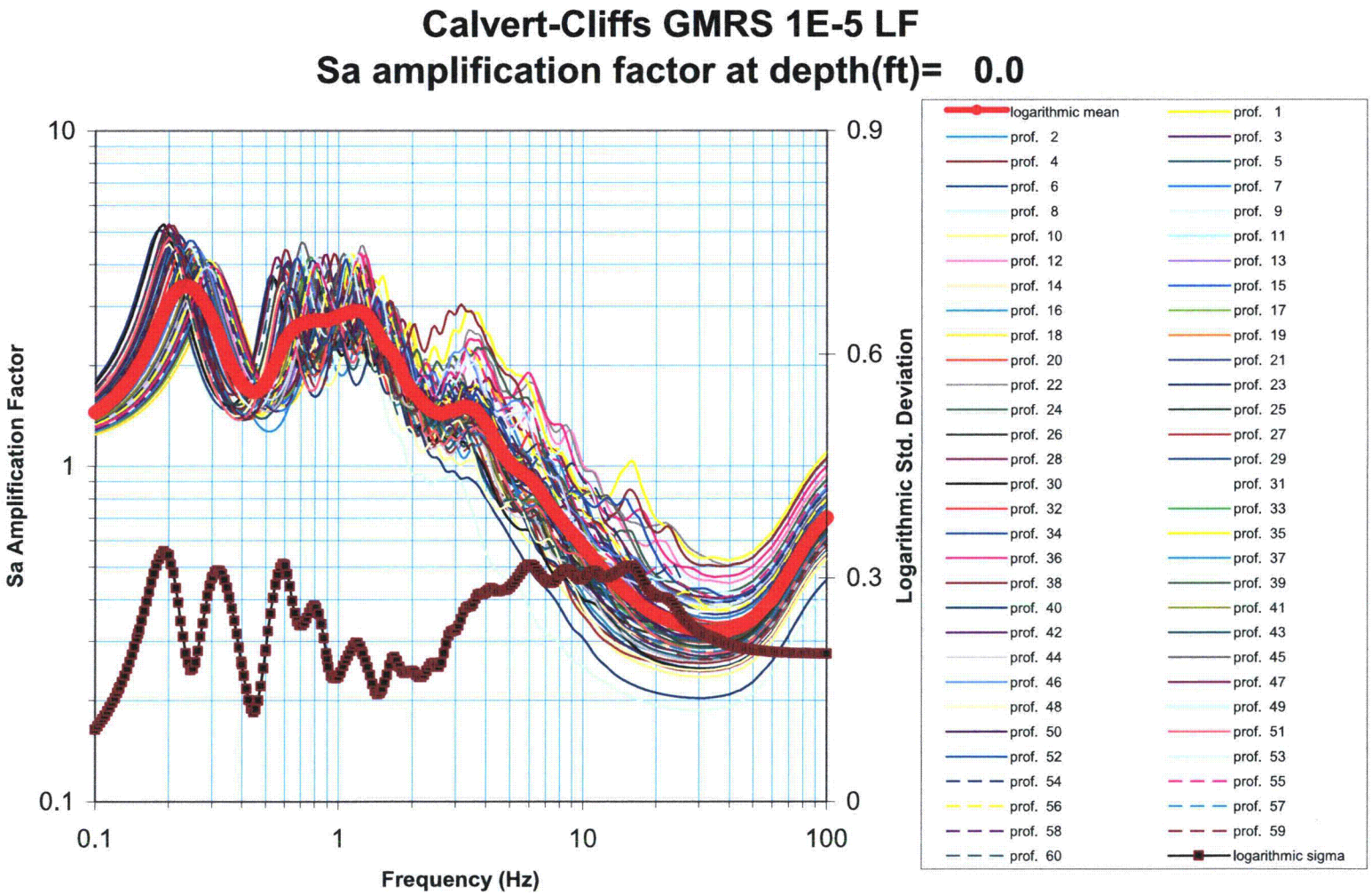

FSAR Section 2.5

Figure 2.5-85—{Maximum Strains vs Depth for 10^{-5} LF Input Motion}

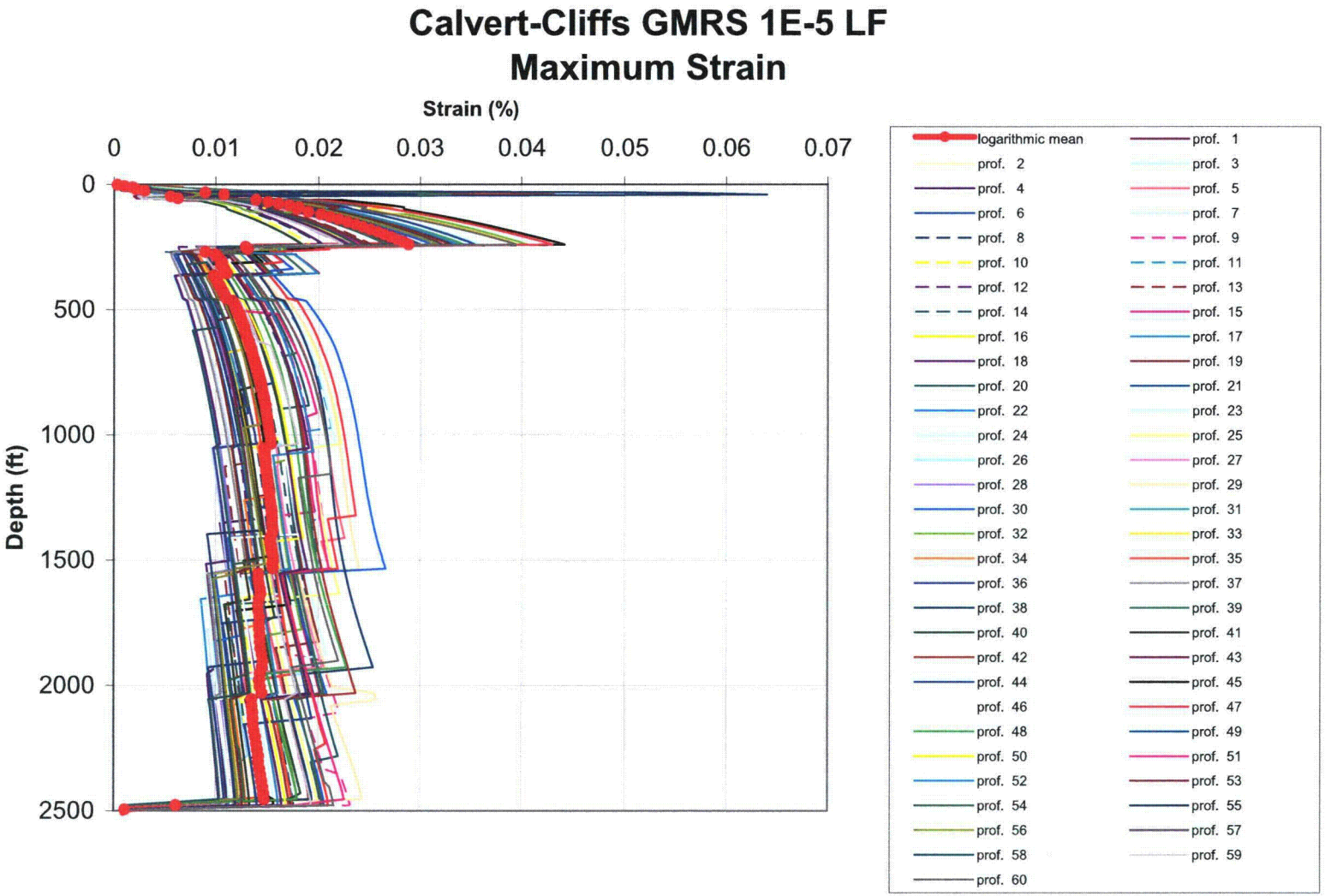

FSAR Section 2.5

Figure 2.5-86—{HF and LF Spectra and Envelopes for 10^{-4} and 10^{-5}}

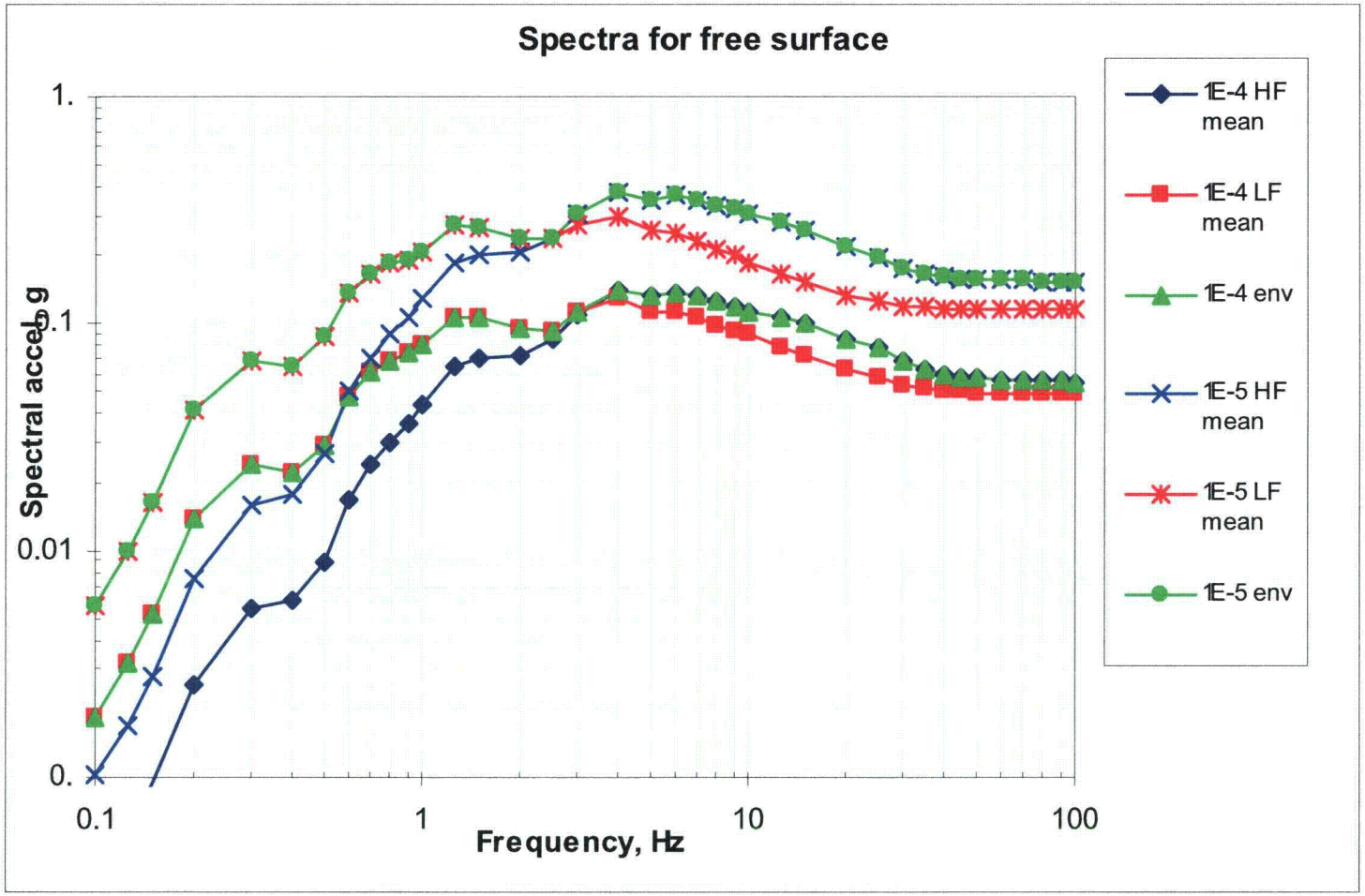

FSAR Section 2.5

Figure 2.5-87—{Recommended Horizontal and Vertical SSE Spectra}